

Simulation of Shocked Acoustic Wave Using DRP Scheme

Khalid M. HOSNY, Ismail A. ISMAIL and
Awatef A. HAMED

Abstract: Numerical simulation of a very small amplitude and high frequency sound wave superimposed on steady flow in a quasi-one dimensional convergent-divergent nozzle is performed using the optimized 7-point central DRP scheme with artificial damping terms. We use both the characteristic and radiation boundary conditions for the boundary treatment. This study contains two different cases; where is no shock in the nozzle, and in the second a normal shock is considered in the divergent section of the nozzle. The acoustic-shock wave interaction is considered.

1- Introduction

Aeroacoustics is the part of fluid dynamics, which is concerned, with the study of all aspects of sound generation and propagation by unsteady flows. In fluid field, noise (sound) is generated by time-dependent fluctuations associated with pressure fluctuations. These pressure fluctuations propagate for long distances to the far field producing the radiated sound (acoustic field).

Reduction of noise is a very serious matter in all aspects of our life. It is a critical point in a wide range of military applications such as ships and submarines operation and object detection. It is important matter in many industrial applications including turbo-machinery, rotorcraft and jet

engines, also, in the civil life and according to the new standard level of allowable noise in the urbane areas.

Computational aeroacoustics is a relatively new and rapidly growing field of research that combines the traditional disciplines of aeroacoustics and computational fluid dynamic. One of the main goals of this new field is to employ the tremendous progress in the computational techniques to overcome the problem of sound (noise) emission from aircraft engines and the other transportation vehicles. Acoustic-shock waves interaction is one of the challenges of the computational aeroacoustics, where the considered numerical method must capture the shock wave and successfully preserve the sound waves that have a very high frequency.

In this work, we perform numerical simulation of a very small amplitude acoustic wave that incident on the inlet of quasi-one dimensional convergent-divergent nozzle. In the solution procedure we employed the optimized high-order 7-points central DRP scheme [1] for spatial derivatives approximations and the optimized four-level time advancing scheme of Adams-Bashforth. The DRP scheme is a non-dissipative scheme where it has a very little dissipation, so, for nonlinear and wave propagation problems it must be combined with an explicit numerical damping terms. We use additional damping terms according to the damping model developed by Tam et al [2,3]. Through the next sections we present the numerical solution of the considered problem with different boundary treatments and discuss the effect of these treatments on the amount of damping needed to suppress the spurious waves.

2- Benchmark Problem

The considered problem is selected from the workshop on benchmark problem [4]. In this problem, the amplitude of the incident waves is specified to be in the order of 10^{-6} times the dynamic pressure that is based on the speed of sound of the incoming flow. The area of the considered nozzle is given by the following function

$$A(x) = \begin{cases} 134 & , -200 \leq x \leq -100 \\ 117 - 17 \cos\left(\frac{\pi x}{100}\right) & , -100 \leq x \leq 19 \\ 97.2 + 0.3x & , 19 \leq x \leq 80 \end{cases} \quad (1)$$

Where, $-200 \leq x \leq 80$ is the computational domain.

The governing equations are the quasi-one dimensional Euler equations, which are casted as follows:

$$\frac{\partial(\rho A)}{\partial t} + \frac{\partial(\rho u A)}{\partial x} = 0 \quad (2.a)$$

$$\rho \left(\frac{\partial u}{\partial t} + u \frac{\partial u}{\partial x} \right) + \frac{\partial p}{\partial x} = 0 \quad (2.b)$$

$$\frac{\partial(\rho A)}{\partial t} + \frac{\partial(\rho u A)}{\partial x} + (\gamma - 1)p \frac{\partial(u A)}{\partial x} = 0 \quad (2.c)$$

The equation of state is

$$p = (\gamma - 1) \rho \left(E - \frac{1}{2} u^2 \right) \quad (3)$$

where ρ, u, p and E are density, velocity, pressure and the total specific energy respectively. γ is the ratio of specific heats where it has the constant value 1.4. Upstream the nozzle ($x \leq -200$), the incoming acoustic wave is specified by

$$\begin{bmatrix} u \\ p \\ \rho \end{bmatrix} = \begin{bmatrix} M \\ 1 \\ \gamma \\ 1 \end{bmatrix} + \begin{bmatrix} 1 \\ 1 \\ 1 \end{bmatrix} \varepsilon \text{Sin} \left[\omega \left(\frac{x}{1+M} - t \right) \right] \quad (4)$$

where:

$M = 0.5$ is the Mach number.

$\varepsilon = 10^{-6}$ is the amplitude of the acoustic waves.

$\omega = 0.1\pi$ is the angular frequency of the acoustic waves.

It is important to use a conservative form of the governing equations. Therefore we replace the primitive variable group (ρ, u, p) by the conservative variable group $(\rho, \rho u, \rho E)$ through the governing equations (2) and the equation of state (3). Since the nozzle cross sectional area $A(x)$ is independent of time, and for the governing equations to be easy to use with the time advancing numerical schemes we do some algebraic procedures and then write the governing equations in the conservative form as follows:

$$\frac{\partial \rho}{\partial t} + \frac{\partial(\rho u)}{\partial x} + \frac{(\rho u)}{A} \frac{dA}{dx} = 0 \quad (5.a)$$

$$\frac{\partial(\rho u)}{\partial t} + \frac{\partial}{\partial x} \left(\frac{3-\gamma}{2} \frac{(\rho u)^2}{\rho} + (\gamma-1)(\rho E) \right) + \frac{(\rho u)^2}{\rho A} \frac{dA}{dx} = 0 \quad (5.b)$$

$$\begin{aligned} \frac{\partial(\rho E)}{\partial t} + \frac{\partial}{\partial x} \left(\gamma \frac{(\rho E)(\rho u)}{\rho} - \frac{(\gamma-1)(\rho u)^3}{2\rho^2} \right) \\ + \frac{1}{A} \left(\gamma \frac{(\rho E)(\rho u)}{\rho} - \frac{(\gamma-1)(\rho u)^3}{2\rho^2} \right) \frac{dA}{dx} = 0 \end{aligned} \quad (5.c)$$

2-1 Normal Shock

The normal shock represents a sudden, almost discontinuous change in fluid properties, which takes place in the direction of the flow. From the thermodynamics point of view, the shock process is irreversible and adiabatic. The second law of thermodynamics, for an irreversible process is $dS > \delta Q/T$, however, for a shock process $\delta Q = 0$, hence

$dS > 0$, which means that the entropy must increase across the shock. From the physical standpoint, the flow ahead of a normal shock wave must be supersonic (Mach number must exceed the unity). According to Prandtl relation the flow behind the normal shock wave must be subsonic (Mach number less than the unity). It is important to mention that shock is a very thin region so that, it can occur in a varying area ducts such as convergent-divergent nozzles.

The normal shock equations can be found in any textbook of gas dynamics. For isentropic gas with constant specific heats, consider M_1 is the Mach number upstream the shock (pre-shock Mach number) and M_2 is the Mach number downstream the shock (post-shock Mach number). John [5] has described the normal shock equations as functions of M_1 and the constant ratio of specific heats γ as follows:

$$M_2^2 = \frac{M_1^2 + \frac{2}{\gamma - 1}}{\frac{2\gamma}{\gamma - 1} M_1^2 - 1}, \quad p_2 = p_1 \left(\frac{2\gamma M_1^2}{\gamma + 1} - \frac{\gamma - 1}{\gamma + 1} \right) \quad (6)$$

$$\rho_2 = \rho_1 \left(\frac{(\gamma + 1)M_1^2}{(\gamma - 1)M_1^2 + 2} \right), \quad u_2 = u_1 \left(\frac{(\gamma + 1)M_1^2 + 2}{(\gamma - 1)M_1^2} \right)$$

2-2 Acoustic-Shock Waves Interactions

Aeroacoustics problems are concerned with aircraft's noise such as jet noise and sonic boom. Thus, for good performance aspects of aircraft design it is important to know noise sources and try to reduce them. One of the important sources of the aircraft's noise is shock wave. Shock waves can be formed in jet flows, jet engines, on airfoils and in supersonic combustion inlets. The presence of the shock waves has strong effect on the noise generation. The effects of shock waves on acoustic waves and correspondingly, effects of acoustic waves on shocks

(i.e. oscillations) or in other words the generation and amplification of acoustic waves by shocks, is usually called acoustic-shock waves interactions.

Based on the linearized theory [6] we will discuss the generation and amplification of acoustic waves by shocks. For a flow field containing nonlinear features such as shock waves, the presence of these waves in the flow, makes it possible for an acoustic wave incident upon a shock to suddenly change its amplitude. Linearized analysis of the interaction of small disturbance with shock wave has been made independently by different investigators such as Powell [7]. Landau and Lifschitz [8] report that the ratio of transmitted to incident acoustic waves determined by the linear theory is:

$$\frac{\delta p_2}{\delta p_1} = \frac{(M_1+1)}{(M_2+1)} * \frac{2(\gamma-1)M_1M_2^2(M_1^2-1) - (M_1+1)[(\gamma-1)M_1^2+2]}{2(\gamma-1)M_2^2(M_1^2-1) - (M_2+1)[(\gamma-1)M_1^2+2]} \quad (7)$$

Where M_1 is the Mach number upstream of the shock (pre-shock Mach number), M_2 is the Mach number downstream of the shock (post-shock Mach number), and γ is the ratio of specific heats of the fluid. The formula (7) predicts amplification of the acoustic wave as it propagates through the shock wave for all pre-shock Mach numbers. Across the shock both of the ratio of the perturbation pressure $\delta p_2/\delta p_1$ and the ratio of the static pressure p_2/p_1 will increase differently.

3- Initial Solutions

Inappropriate or crude initial conditions used in computational aeroacoustics can produce large initial transients, where, sharp transients can generate spurious waves as the acoustic waves propagate to the far field. Therefore, it is important to use initial conditions that are as close as possible to the exact solution to avoid or at least minimize the initial transients. In this problem we will use the mean solution (computed by integrating the steady-state governing equations analytically [4]) as initial solution. We can get the mean solution after the following steps:

First step

We will compute fluid flow variables at the nozzle throat by using the following equations:

$$\rho_*^{\gamma+1} \left(\frac{A_*}{A_1} \right)^2 + \frac{2}{\gamma+1} = \frac{\gamma+1}{\gamma-1} \rho_*^{\gamma-1} \quad (8.a)$$

$$p_* = \frac{1}{\gamma} \rho_*^\gamma \quad (8.b)$$

$$u_* = \rho_*^{\frac{\gamma-1}{2}} \quad (8.c)$$

Where the subscript * is used to denote the fluid flow variables at the nozzle throat and A_1 is the cross sectional area of the uniform part of the nozzle.

Equation (8.a) is a nonlinear equation that can be solved numerically [9] to compute the density at the throat, therefore, by using the equation (8.b) and (8.c) we get the other variables at the throat.

Second step

In this step we get the mean flow solution by solving the following equations:

$$\overline{\rho u A} = \rho_* u_* A_* \quad (9.a)$$

$$\frac{\overline{p}}{p_*} = \left(\frac{\overline{\rho}}{\rho_*} \right)^\gamma \quad (9.b)$$

$$\frac{\overline{u}^2}{2} + \frac{\gamma}{\gamma+1} \frac{p_*}{\rho_*^\gamma} (\overline{\rho})^{\gamma-1} = \frac{u_*^2}{2} + \frac{\gamma}{\gamma-1} \frac{p_*}{\rho_*} \quad (9.c)$$

Substitute from (9.a) into (9.c) we get:

$$\bar{u}^2 + \frac{2\gamma}{\gamma+1} \frac{p_*}{\rho_*} (u_* A_*)^{\gamma-1} (\bar{u} A)^{1-\gamma} = u_*^2 + \frac{2\gamma}{\gamma-1} \frac{p_*}{\rho_*} \quad (10)$$

Equation (10) is a nonlinear equation. We can solve this equation numerically to get the mean velocity when the flow variables at the throat are known. Once we have solved this equation, equation (9.a) and (9.b) are used to find the values of mean density and pressure.

The initial flow solutions of the considered nozzle problem in the two different cases are plotted in the figure (2) and (4). Mach numbers in these cases are plotted in figure (3) and (5). From the plotted figures, it is clear that both of pressure and density increase across the shock while the velocity and Mach number decrease.

4- Spatial Discretization

The optimized 7-point central finite difference DRP scheme presents a fourth-order spatial derivative approximation. For a function f , the approximation of the spatial derivative $\partial f / \partial x$ at the node l is defined as follows:

$$\left(\frac{\partial f}{\partial x} \right)_l \cong \frac{1}{\Delta x} \sum_{j=-3}^3 a_j f_{l+j} \quad (11)$$

Where:

Δx is the mesh spacing.

l is integer.

a_j are the coefficients of the scheme.

$$\begin{aligned} a_0 &= 0 & a_1 &= -a_{-1} = 0.770882380518 \\ a_2 &= -a_{-2} = -0.166705904415 & & (12) \\ a_3 &= -a_{-3} = +0.0208431427703 \end{aligned}$$

5- Time Marching Scheme

In our computations we use the optimized multi-levels time advancing scheme of Adams-Bashforth. To explain this method, let us rewrite the governing equations of the considered problem in the following compact form

$$\frac{\partial U}{\partial t} = F(U) \quad (13)$$

Where U is the vector of the unknowns and $F(U)$ represents the fluxes vector.

By dividing the time axis into uniform grids with a constant time step Δt and assuming that U and it's time derivative are known at different four time levels n , $n-1$, $n-2$ and $n-3$ we can advance the solution to the next time level by using the following four-level finite difference approximation:

$$U^{(n+1)} = U^{(n)} + \Delta t \sum_{j=0}^3 b_j \left(\frac{\partial U}{\partial t} \right)^{(n-j)} \quad (14)$$

Where values of the coefficients b_j are [10]:

$$\begin{aligned} b_0 &= 2.3025580888 & b_1 &= -2.4910075998 \\ b_2 &= 1.5743409332 & b_3 &= -0.3858914222 \end{aligned}$$

6- Artificial Damping Method

The spurious (high-frequency) waves are pollutants of the numerical solution and have a critical effect on the quality of this solution. Therefore, to obtain a high quality numerical solution, it should be free from all the numerical spurious waves. The optimum way to get such solution is to damp the spurious waves as soon as they are generated. This can be achieved by using an artificial damping method. In the

considered problem we will use Tam damping method. In this method we can add explicit numerical damping terms to the difference equations where the value of the additional terms can be controlled by a free parameter. The numerical values of the weight coefficients are:

7-Points Stencil

$$\begin{aligned} d_0 &= 0.327698660845 & d_1 &= d_{-1} = -0.235718815308 \\ d_2 &= d_{-2} = 0.086150669577 & d_3 &= d_{-3} = -0.014281184692 \end{aligned}$$

5-Points Stencil

$$\begin{aligned} d_0 &= 0.375 & d_1 &= d_{-1} = -0.25 \\ d_2 &= d_{-2} = 0.0625 \end{aligned}$$

3-Points Stencil

$$d_0 = 0.5 \quad d_1 = d_{-1} = -0.25$$

7- Solution Procedures

According to the requirements of the time marching scheme, we consider the following:

$$\frac{\partial \rho}{\partial t} = K_1, \quad \frac{\partial(\rho u)}{\partial t} = K_2 \quad \text{and} \quad \frac{\partial(\rho E)}{\partial t} = K_3$$

Discretizing the governing equations in its conservative form using the DRP scheme and explicit damping terms with damping coefficient \mathfrak{R} , we get the following equations

$$(K_1)_t^{(n)} = -\frac{1}{\Delta x} \sum_{j=-3}^3 a_j (\rho u)_{t+j}^{(n)} - \frac{1}{\Delta x} \left(\frac{\rho u}{A} \right)_t^{(n)} \sum_{j=-3}^3 a_j A_{t+j} - \mathfrak{R} \sum_{j=-3}^3 d_j (\rho)_{t+j}^{(n)} \quad (15.a)$$

$$\begin{aligned}
(K_2)_\ell^{(n)} = & -\frac{1}{\Delta x} \sum_{j=-3}^3 a_j \left(\frac{3-\gamma}{2} \frac{(\rho u)^2}{\rho} + (\gamma-1)(\rho E) \right)_{\ell+j}^{(n)} \\
& - \frac{1}{\Delta x} \left(\frac{(\rho u)^2}{\rho A} \right)_\ell^{(n)} \sum_{j=-3}^3 a_j A_{\ell+j} - \Re \sum_{j=-3}^3 d_j (\rho u)_{\ell+j}^{(n)}
\end{aligned} \tag{15.b}$$

$$\begin{aligned}
(K_3)_\ell^{(n)} = & -\frac{1}{\Delta x} \sum_{j=-3}^3 a_j \left(\gamma \frac{(\rho E)(\rho u)}{\rho} - (\gamma-1) \frac{(\rho u)^3}{\rho^2} \right)_{\ell+j}^{(n)} \\
& - \frac{1}{\Delta x A} \left(\gamma \frac{(\rho E)(\rho u)}{\rho} - (\gamma-1) \frac{(\rho u)^3}{\rho^2} \right)_\ell^{(n)} \sum_{j=-3}^3 a_j A_{\ell+j} - \Re \sum_{j=-3}^3 d_j (\rho E)_{\ell+j}^{(n)}
\end{aligned} \tag{15.c}$$

The four-level time marching scheme for the governing equations in the conservative form can be written as follows

$$\rho_\ell^{(n+1)} = \rho_\ell^{(n)} + \Delta t \sum_{j=0}^3 b_j (K_1)_\ell^{(n-j)} \tag{16.a}$$

$$(\rho u)_\ell^{(n+1)} = (\rho u)_\ell^{(n)} + \Delta t \sum_{j=0}^3 b_j (K_2)_\ell^{(n-j)} \tag{16.b}$$

$$(\rho E)_\ell^{(n+1)} = (\rho E)_\ell^{(n)} + \Delta t \sum_{j=0}^3 b_j (K_3)_\ell^{(n-j)} \tag{16.c}$$

The boundary points have special treatments according to extrapolation. Based on information in [10] we will write the coefficients of the DRP scheme for the boundary points as follows:

(I) Left Boundary Points $\ell = 0, \ell = 1, \ell = 2$

The point $\ell = 0$:

There are no points to left and six points to right. The coefficients are:

$$\begin{array}{ll} a_0 = -2.192280339 & a_4 = -2.833498741 \\ a_1 = 4.748611401 & a_5 = 1.128328861 \\ a_2 = -5.108851915 & a_6 = -0.203876371 \\ a_3 = 4.461567104 & \end{array}$$

The point $\ell = 1$:

There is one point to left and five points to right. The coefficients are:

$$\begin{array}{ll} a_{-1} = -0.209337622 & a_3 = 0.768949766 \\ a_0 = -1.084875676 & a_4 = -0.281814650 \\ a_1 = 2.147776050 & a_5 = 0.048230454 \\ a_2 = -1.388928322 & \end{array}$$

The point $\ell = 2$:

There are two points to left and four points to right. The coefficients are:

$$\begin{array}{ll} a_{-2} = 0.049041958 & a_2 = -0.518484526 \\ a_{-1} = -0.468840357 & a_3 = 0.166138533 \\ a_0 = -0.474760914 & a_4 = -0.026369431 \\ a_1 = 1.273274737 & \end{array}$$

(II) Right Boundary Points $\ell = N, \ell = N-1, \ell = N-2$

The right boundary points are the same as the left ones but with negative sign.

8- Boundary Conditions Treatment

Proper boundary conditions implementation is important for an accurate numerical solution. For the nozzle problem under consideration, the boundary conditions are divided into inflow and outflow boundary conditions. Inflow boundary conditions must allow the incoming acoustic waves to propagate into the computational domain. Also, the inflow boundary conditions must permit the reflected waves to leave the computational domain. The outflow boundary condition must allow the outgoing acoustic waves to pass without introducing non-physical reflections to the computational domain.

8-1 Characteristic Boundary conditions

There are many approaches for boundary conditions treatment [11]. One of these approaches is the Thompson non-reflecting boundary condition [12,13] based on the theory of characteristic. The main idea of the Thompson non-reflecting boundary conditions is that, he considers the amplitude of the incoming waves in the computational domain equal to zero (no incoming waves) and then computes the outgoing waves using backward difference from the interior of the computational domain. Therefore, we can not apply Thompson non-reflecting boundary conditions as it is, but we must use modified non-reflecting boundary conditions that allow the incoming acoustic wave to propagate through the computational domain. To achieve this goal we will consider non-zero incoming acoustic waves. Now we will discuss in details the implementation of the non-reflecting boundary conditions on the considered nozzle problem.

According to the theory of characteristics the compatibility equations of the original governing equations (5) can be written in the following form

$$\frac{\partial p}{\partial t} - \rho c \frac{\partial u}{\partial t} + (u-c) \left(\frac{\partial p}{\partial x} - \rho c \frac{\partial u}{\partial x} \right) + \frac{\rho u c^2}{A} \frac{\partial A}{\partial x} = 0 \quad (R1)$$

$$\frac{\partial p}{\partial t} - c^2 \frac{\partial \rho}{\partial t} + u \left(\frac{\partial p}{\partial x} - c^2 \frac{\partial \rho}{\partial x} \right) = 0 \quad (R2)$$

$$\frac{\partial p}{\partial t} + \rho c \frac{\partial u}{\partial t} + (u + c) \left(\frac{\partial p}{\partial x} + \rho c \frac{\partial u}{\partial x} \right) + \frac{\rho u c^2}{A} \frac{\partial A}{\partial x} = 0 \quad (R3)$$

According to Thompson notation we write the following

$$H_1 = (u - c) \left(\frac{\partial p}{\partial x} - \rho c \frac{\partial u}{\partial x} \right) \quad (17.a)$$

$$H_2 = u \left(\frac{\partial p}{\partial x} - c^2 \frac{\partial \rho}{\partial x} \right) \quad (17.b)$$

$$H_3 = (u + c) \left(\frac{\partial p}{\partial x} + \rho c \frac{\partial u}{\partial x} \right) \quad (17.c)$$

After some algebraic manipulation procedures we can write the compatibility equations in the following form:

$$\frac{\partial p}{\partial t} = -\frac{1}{2} [H_1 + H_3] - \frac{\rho u c^2}{A} \frac{\partial A}{\partial x} \quad (18.a)$$

$$\frac{\partial u}{\partial t} = \frac{1}{2\rho c} [H_1 - H_3] \quad (18.b)$$

$$\frac{\partial \rho}{\partial t} = \frac{1}{c^2} \left[\frac{\partial p}{\partial t} + H_2 \right] \quad (18.c)$$

Inflow Boundary Conditions

For the considered nozzle problem, the inflow boundary condition is always subsonic. According to the discussion of Anderson [14] there

are left-running characteristics, which, represent an outgoing waves and a right- running characteristics, which, represent an incoming waves. R_2 and R_3 represent an incoming entropy and acoustic waves, while, R_1 represents an outgoing acoustic wave. The area of inlet of the nozzle has a constant value, so, the spatial derivative of the area must equal to zero ($\partial A/\partial x=0$).

In this method, the spatial derivatives along the outgoing characteristic H_1 are computed in the interior using the backward differencing, while, the spatial derivatives along the incoming characteristic H_3 are computed from the analytical expressions of the incoming acoustic wave described by the equations (4). Since there is no incoming entropy waves we consider H_2 equal to zero. We write incoming characteristic H_3 in the following form

$$H_3 = (u + c)(1 + \rho c) \frac{\varepsilon \omega}{M+1} \cos \left[\omega \left(\frac{x}{M+1} - t \right) \right] \quad (19)$$

As we have discussed before it is better to use the conservative form of the governing equations, therefore, we will use the conservative and primitive time derivative relation's [12]. We turn the boundary equations into its conservative form as follows,

$$\frac{\partial \rho}{\partial t} = \frac{\partial \rho}{\partial t} \quad (20.a)$$

$$\frac{\partial(\rho u)}{\partial t} = u \frac{\partial \rho}{\partial t} + \rho \frac{\partial u}{\partial t} \quad (20.b)$$

$$\frac{\partial(\rho E)}{\partial t} = \frac{1}{2} u^2 \frac{\partial \rho}{\partial t} + \rho u \frac{\partial u}{\partial t} + \frac{1}{\gamma - 1} \frac{\partial p}{\partial t} \quad (20.c)$$

Outflow Boundary Conditions

The considered nozzle problem has two different cases for the outflow boundary conditions. The first one, is supersonic outflow boundary conditions and the other one, is subsonic boundary conditions.

(I) Supersonic outflow boundary conditions:

If the flow at the nozzle exit is supersonic, this means that all of the waves are forced to move out of the computational domain. Therefore, the compatibility and the original governing equations are identical. The spatial derivatives of all the governing equations are discretized with backward differences.

(II) Subsonic outflow boundary conditions:

When the nozzle exit pressure increases, a shock is formed in the divergent part of the nozzle. In this case, the outflow at the nozzle exit is subsonic with the acoustic perturbations. Based on the analysis of the characteristic theory, there are two outgoing characteristic waves and one incoming characteristic wave. The outgoing waves are the acoustic wave with the velocity $(u + c)$ and the entropy wave of the velocity u (the entropy wave formed inside the nozzle). The incoming wave is the acoustic wave with the velocity $(u - c)$. According to the idea of non-reflecting boundary conditions of Thomson, we must suppress the incoming acoustic wave. To do so we consider the compatibility equations $R2$ and $R3$ and instead of the compatibility equations $R1$ we use the following equation

$$\frac{\partial P}{\partial t} - \rho c \frac{\partial u}{\partial t} = 0 \quad (21)$$

(8-2) Radiation Boundary Conditions

At the left boundary of the computational domain for the considered nozzle problem we can apply the radiation boundary condition of Tam and Webb [15]. Radiation boundary conditions will allow the

incoming acoustic wave to propagate into the computational domain and at the same time permit the reflected waves to leave the computational domain without reflections. As we discussed before, the radiation boundary conditions are derived from the asymptotic solutions of the governing equations.

For the current problem, the following equations represent non-homogeneous radiation boundary conditions that can be applied at the left boundary. The equations are

$$\frac{\partial}{\partial t} \begin{pmatrix} \rho \\ u \\ p \end{pmatrix} = (1-M) \frac{\partial}{\partial x} \begin{pmatrix} \rho \\ u \\ p \end{pmatrix} - \begin{pmatrix} 1 \\ 1 \\ 1 \end{pmatrix} \frac{2\omega\varepsilon}{(1+M)} \cos \left[\omega \left(\frac{x}{1+M} - t \right) \right] \quad (22)$$

where:

M is the Mach number of the incoming acoustic wave.

ω is the angular frequency.

ε is the amplitude of the incoming acoustic wave.

x represents the position of the left boundary.

9- Results and Discussion

Numerical simulation of acoustic wave incident on steady flows with or without normal shock inside a quasi-one dimensional convergent-divergent nozzle shown on figure (1) is performed using the 7-point central DRP scheme for spatial derivatives and the four-level time advancing scheme for time derivatives. In the discretization of the conservative governing equations we use explicit damping terms in order to suppress the spurious waves generated during the computations.

A steady-state solution is obtained until residuals are driven to machine zero. After the steady state is achieved we consider the incidence of the acoustic wave defined by the equation (4) on the inlet of the nozzle ($x = -200$). We perform the problem with two different cases, the first one is without shock and the second one is where a normal shock is formed in the divergent section of the nozzle.

In the first case, the inflow boundary conditions are subsonic (Mach number equal to 0.5). For the boundary condition treatments we consider the characteristic boundary conditions of Thompson and the radiation boundary conditions of Tam. The outflow boundary conditions are supersonic (Mach number equals 1.55) so, no special treatments are needed. We used the 7-point of Tam's damping method for the interior points and both 5- and 3-points for the other points in the computational domain. No damping is used for the terminal points ($x = -200$ & $x = 80$). The damping coefficient is a free parameter used to control the damping terms. The small damping can not suppress the spurious waves and on the other hand the high damping values has a harmful effect on the acoustic waves. Therefore, we can say that, the damping coefficient plays the key role in the success of the computation. In our computation we use the value 0.9 for the damping coefficient. Figure (6) shows three snapshots of the spatial distribution of pressure perturbations.

In the second case, normal shock is formed in the nozzle by increasing the exit pressure with respect to the total inlet pressure. The inflow boundary conditions are subsonic (Mach number equals 0.5). As in the first case, we consider the characteristics boundary conditions of Thompson and the radiation boundary conditions of Tam for the boundary condition treatments. The outflow boundary conditions are subsonic (Mach number equals to 0.6). We use the characteristic boundary conditions of Thompson. Unlike the first case, the constant damping coefficient can not be a good selection. In this case we use a pressure sensor to locate where the greatest pressure gradient is and then choose the value of the damping coefficient consequently. We use the 3-point of Tam's damping method for all points of the computational domain where no damping is used for the terminal points ($x = -200$ & $x = 80$). In the computation of this case we use the value 0.65 for the damping coefficient and increase it to 4.5 around the greatest pressure gradient. Figure (7) shows two snapshots of the spatial distribution of pressure perturbations in presence of the normal shock. From figure (8) we see very good agreement between the exact mean pressure (represents by line) and the numerical one (represents by bold black circles).

From the previous discussion we conclude that the DRP scheme with a careful selection of the damping terms perform the problem very

well. According to the little dissipation of this scheme the convergence to the steady state is a slow convergence where the computation requires approximately 40000 times the time increment Δt in the case without shock and more than double of this number for the computation in the case of shock. For more discussion and numerical solutions of a similar problem containing an acoustic wave interact with a shock in a nozzle we refer to the references [16,17].

References

- 1- Tam, C.K.W. and Webb, C.J., (1993) "Dispersion-Relation-Preserving Finite Difference Scheme for Computational Acoustics" *Journal Computational Physics*, Vol.107, pp. 262-281.
- 2- Tam, C.K.W. and Shen, H., (1993) "Direct Computation of Nonlinear Acoustic Pulses Using High Order Finite Difference Schemes" AIAA Paper 93-4325.
- 3- Tam, C.K.W., Webb, C.J. and Zhong Dong, (1993) "A Study of the Short Wave Components in Computational Acoustics" *Journal of Computational Acoustics*, Vol. 1, pp. 1-30.
- 4- Hardin, J.C., Ristorcelli, J.R. and Tam, C.K.W., (Editors), (1995) "First ICASE/LaRC Workshop On Benchmark Problems in Computational Aeroacoustics" (Hampton, VA), NASA CP. 3300.
- 5- James E.A. John, (1984) "Gas Dynamics" second edition, Prentice-Hall.
- 6- Meadows, K.R., Casper, J. and Caughey, D.A., (1993) "A Numerical Investigation of Sound Amplification by a Shock Wave" *Computational Aero- and Hydro-Acoustics*, FED-ASME, Vol. 147, pp. 47-52.
- 7- Powell, A., (1959) "One-dimensional Treatment of Weak Disturbances of Shock Wave" *Aeronautical Research Council Current Papers*, CP. 441.
- 8- Landau and Lifschitz (1959) "Fluid Mechanics" Pergamon Press, New York.
- 9- Curtis F. Gerald, and Patrick O. Wheatley, (1988) "Applied Numerical Analysis" Fourth Edition, Addison Wesley.
- 10- Tam, C.K.W., (1995) "Computational Aeroacoustics: Issues and Methods" *AIAA Journal*, Vol. 33, pp. 1788-1796.

- 11- Tam, C.K.W., (1997) "Advances in Numerical Boundary Conditions for Computational Aeroacoustics" AIAA paper 97-1774.
- 12- Thompson, K.W., (1987) "Time-Dependent Boundary Conditions for Hyperbolic System" Journal of Computational Physics, Vol. 68, pp. 1-24.
- 13- Thompson, K.W., (1990) "Time-Dependent Boundary Conditions for Hyperbolic System, II" Journal of Computational Physics, Vol. 89, pp. 439-461.
- 14- Anderson, J.D., (1995) "Computational Fluid Dynamics: the basics with applications" McGraw-Hill, Inc., New York.
- 15- Tam, C.K.W., and Zhong Dong, (1996) "Radiation and Outflow Boundary Conditions for Direct Computation of Acoustic and Flow Disturbances in a Nonuniform Mean Flow" Journal of Computational Acoustics, Vol. 4, pp. 175-201.
- 16- Meadows, K.R., Casper, J. and Caughey, D.A., (1994) "Computing Unsteady Shock Waves for Aeroacoustic Applications" AIAA Journal, Vol.32, pp. 360-1366.
- 17- Bui, T.T. and Mankbadi, R.R., (1998) "Direct Numerical Simulation of Acoustic Waves Interacting With A Shock Wave In A Quasi-1D Convergent-Divergent Nozzle Using Unstructured Finite Volume Algorithm" International Journal of Computational Fluid Dynamics, Vol. 10, pp. 281-298.

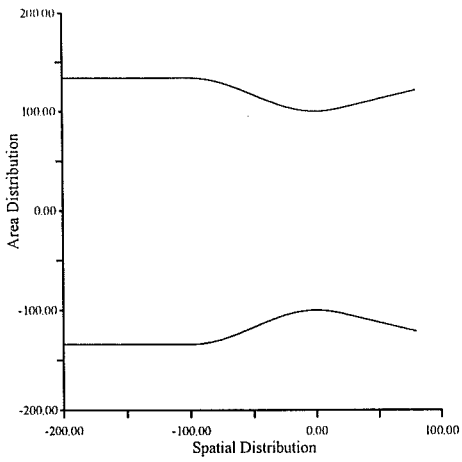


Fig. (1): Nozzle Geometry

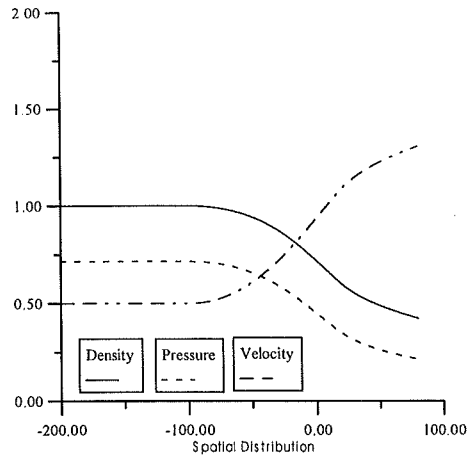


Fig. (2): Initial Steady-State Solutions (Without shock)

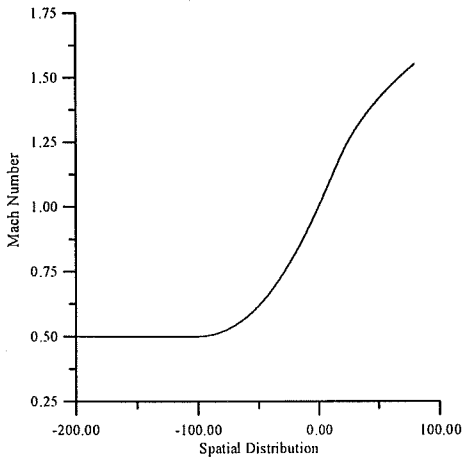


Fig. (3): Mach Number (Without shock)

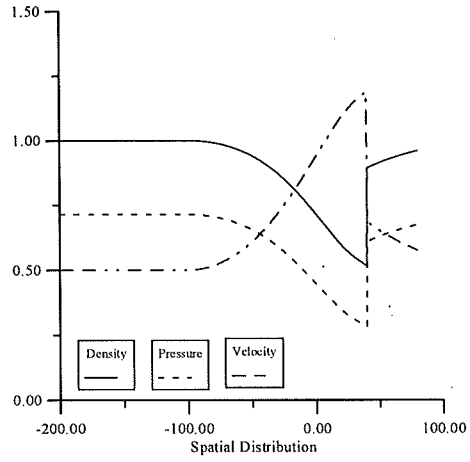


Fig. (4): Initial Steady State Solutions (With shock)

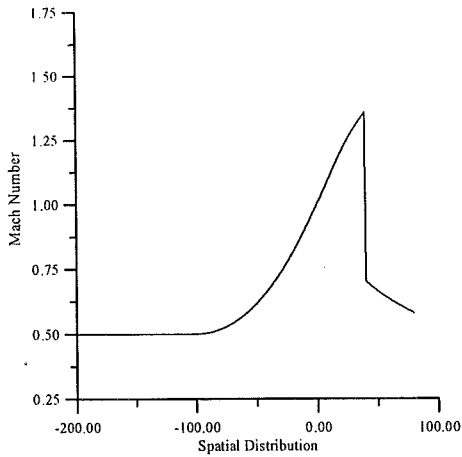


Fig. (5): Mach Number
(With shock)

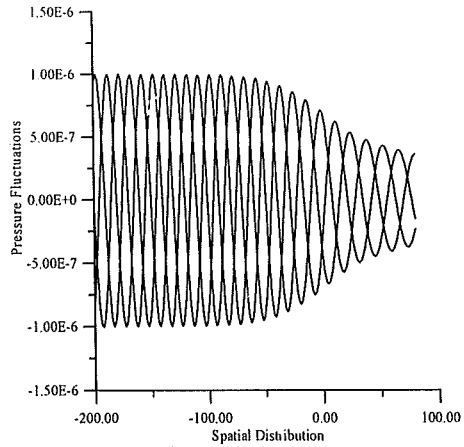


Fig. (6): Three Snapshots of Pressure
Fluctuations (Without shock)

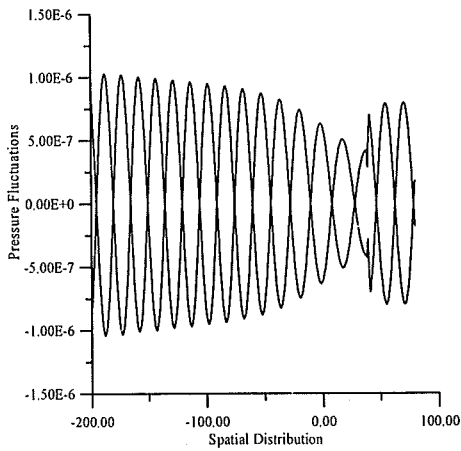


Fig. (7): Two Snapshots of Pressure
Fluctuations (With shock)

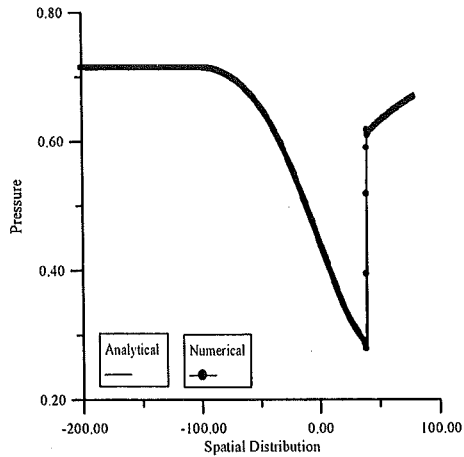


Fig. (8): Numerical & Analytical
Mean Pressure (With shock)

Khalid M. Hosny , Ismail A. Ismail
College of Computers and Informatics,
Zagazig University, Zagazig, Egypt.
e.mail: k_hosny@yahoo.com

Awatef A. Hamed
Aerospace Engineering & Engineering
Mechanics Department, College of
Engineering, University of Cincinnati,
Cincinnati 45219-0070, Ohio, USA.
e.mail: ahamed@uc.edu